Chemical Absorption of Gas into Liquid Film on Rotating Drum

AUTHOR(S):

OISHI, Tetsuo; YAMAGUCHI, Iwao; NAGATA, Shinji

CITATION:

OISHI, Tetsuo ...[et al]. Chemical Absorption of Gas into Liquid Film on Rotating Drum. Memoirs of the Faculty of Engineering, Kyoto University 1965, 27(3): 317-346

ISSUE DATE:

1965-08-31

URL:

http://hdl.handle.net/2433/280633

Chemical Absorption of Gas into Liquid Film on Rotating Drum

By

Tetsuo OISHI*, Iwao YAMAGUCHI** and Shinji NAGATA***

(Received March 31, 1965)

With a rotating drum type gas-liquid contactor of known area, the effects of gas rate and the rotational speed of the drum on the thickness of liquid film were observed and the rate of gas absorption accompanied by a chemical reaction in the liquid phase was measured using either one of the catalysts, mannitol, Cu^{++} and Co^{+++}.

The analytical solution was presented for the simultaneous unsteady state absorption and $(m+1)$-st order reaction (m-th order with reactant A and 1st order with reactant B respectively). Experimental results were compared with theories and the five states of rate controlling were verified which had formerly been derived analytically[18]. The five states correspond to the case where mass transfer are controlled by the resistances of ; (1) chemical reaction in the liquid, (2) both chemical reaction and diffusion in the liquid, (3) diffusion of the dissolved gas in the liquid film, (4) both diffusion and chemical reaction in the liquid film and (5) diffusion of the reactant from the liquid bulk. The rate constant of the accompanied reaction was also determined.

Introduction

The design of a gas-liquid reactor and the determination of optimum operating conditions should be made considering the physical properties and the reaction mechanism of the system which is ordinarily complicated in heterogeneous system. The rate controlling step may consist of a series of resistances to diffusion and chemical reaction.

In practical apparatuses such as agitators, bubble towers and packed towers, *etc.*, the determination of reaction mechanism and rate controlling step are rather difficult, because the flow pattern of the gas and liquid are intricated and the interfacial area is hardly measurable. Hence, the experimental apparatus having the following characteristics are recommended for the theoretical studies.

(a) Interfacial area between gas and liquid is measured accurately.

* Kanegafuchi Chemical Industrial Co., Ltd.
** Department of Engineering, Teijin, Ltd., Osaka Head Office
*** Department of Chemical Engineering

(b) Mass transfer coefficient in the gas phase (k_a) and that in the liquid phase (k_b) are measurable separately in a wide range of reaction conditions.

(c) Effective under high pressure and temperature.

The authors contrived a gas-liquid contactor of a rotating drum type to fit these requirements. Solutions presented by the authors[13] for mass transfer in steady state molecular diffusion followed by a reaction ($A+\nu B \rightarrow R+S$) may be extended to the case of unsteady state diffusion. The rate of chemical absorption in a system consisting both of a diffusion film and a finite volume of homogeneous bulk liquid is observed in the oxidation reaction of sodium sulfite in order to verify the five states of rate controlling. Comparisons are also made with the theoretical analysis and the experimental data. The rate of oxidation of sodium sulfite in aqueous solution by gaseous oxygen, which is largely changed in magnitude by a selection of catalysts, is measured in a wide range of reaction conditions and the reaction mechanism is made clear. The reaction rate constant is also measured.

Experimental Apparatus and Procedures

The reactor is made of transparent methyl-methacrylate resin whose geometry is shown in **Fig. 1.** Liquid is charged from an inlet (a), entrained

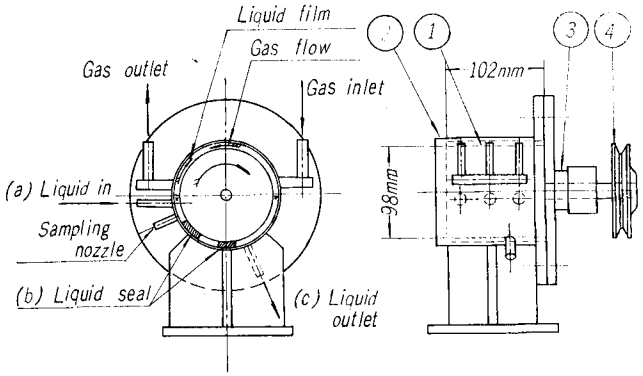

Fig. 1. Rotating drum gas-liquid contactor used.
① : Rotating drum, ② : Casing,
③ : Cover and Bearing, ④ : V-pulley

on the surface of a rotating drum ① and contacts with the gas which flows countercurrently in the spacing between the drum and the casing ②. After absorption of oxygen, the liquid is held back by the liquid seals (b) set on the inside bottom of the casing ② and discharged from the outlet (c). The liquid level at the inlet and outlet is so adjusted that the gas and liquid

contact on the upper half of the drum. An agitation vessel is also used in a special case of reaction rate controll.

Physical Absorption of Oxygen into Water (Liquid Phase Mass Transfer Coefficient: k_b)

In order to estimate the liquid flow rate, F, and the value of k_b, the rate of physical absorption of pure O_2 into water is measured where the diffusion resistance in the liquid phase is effective.

1) Rate of flow and thickness of liquid film

When the liquid seal is imperfect, a small amount of liquid in the chamber, H_2 (refer to **Fig. 2**) leaks into the chamber H_1 whose rate is denoted

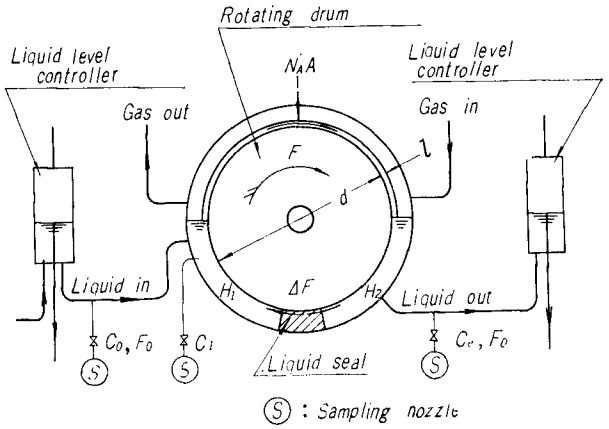

Fig. 2. Concentration of flowing liquid at various parts in contactor.

by ΔF. The rate of liquid entrained on the rotating drum, F, is given as follows:

$$F = F_0 + \Delta F \tag{1}$$

where F_0 is the rate of liquid feed or discharge, hence,

$$C_0F_0 + \Delta FC_e = (F_0 + \Delta F)C_1 \tag{2}$$

From Eqs. (1) and (2),

$$F = \frac{C_e - C_0}{C_e - C_1}F_0 \tag{3}$$

F is determined by measuring the values of C_0, C_1, C_e and F_0 in Eq. (3).

Denoting the thickness of the liquid film; l, the diameter of the drum; d, the width; B and the rotating speed; N, we have,

$$F = \pi \cdot dBlN \tag{4}$$

Hence, l is estimated from Eqs. (3) and (4) as follows:

$$l = \frac{F}{\pi dBN} = \frac{F_0}{\pi dBN}\frac{C_e - C_0}{C_e - C_1} \tag{5}$$

2) Absorption rate equation (Unsteady state absorption into liquid film of finite thickness)

Taking the material balance of the absorbed gas,

$$F_0(C_e - C_0) = N_A A \tag{6}$$

Contact time of gas and liquid τ is given by:

$$\tau = \frac{1}{2N} \tag{7}$$

When N=74~400 r.p.m., τ is equal to 0.406~0.075 sec. In this range of τ, unsteady diffusion takes place. As the liquid moves adhering on the drum surface, the rate of absorption is analysed by the penetration theory proposed by Higbie[8] based on an unsteady state molecular diffusion. As the thickness of the liquid film is comparatively thin, the solution should be given at the condition of a finite thickness.

The concentration distribution in the liquid film is shown in **Fig. 3.**

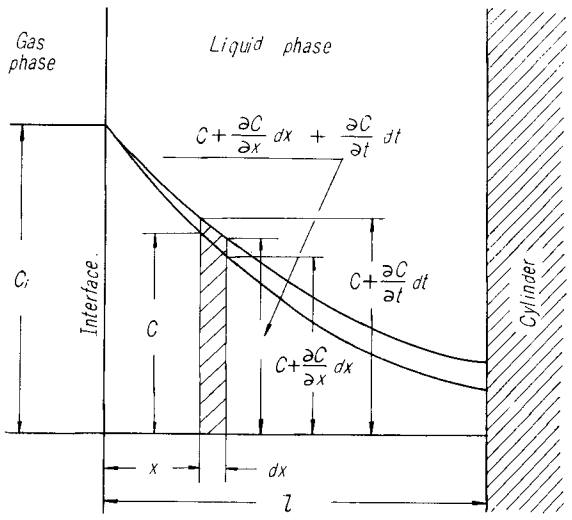

Fig. 3. Concentration distribution.

Taking the material balance at a distance x from the interface and at a time t, we have

$$\frac{\partial C}{\partial t} = D_A \frac{\partial^2 C}{\partial x^2} \tag{8}$$

Initial and boundary conditions are,

$$\left.\begin{aligned} C &= C_1 \quad \text{at } t=0 \text{ and } 0<x<l \\ &\qquad \text{(refer to Fig. 2)} \\ C &= C_i \quad \text{at } t>0 \text{ and } x=0 \\ \frac{\partial C}{\partial x} &= 0 \quad \text{at } t>0 \text{ and } x=l \end{aligned}\right\} \tag{9}$$

Eq. (8) should be solved under the conditions of Eq. (9). The following solution for the contact time of $0\sim\tau$ is obtained.

$$\left.\begin{aligned} N_A &= 2\sqrt{\frac{D_A}{\pi\tau}}(C_i-C_1)(1+S_n) \\ S_n &= 2\sum_{n=1}^{\infty}(-1)^n \exp\left(-\frac{l^2n^2}{\tau D_A}\right) \end{aligned}\right\} \tag{10}$$

Therefore k_b is expressed by the following equation as has been presented by S. Fujita[6].

$$k_b \equiv 2\sqrt{\frac{D_A}{\pi\tau}}(1+S_n) \tag{11}$$

At a higher speed of rotating drum, S_n tends to zero and we have,

$$k_b \equiv 2\sqrt{\frac{D_A}{\pi\tau}} \tag{11'}$$

By substituting Eq. (10) into Eq. (6), we have,

$$k_b = \frac{C_e-C_0}{C_i-C_1}\frac{F_0}{A} \tag{12}$$

3) Conditions and results of experiments

0.1 N aqueous solution of KOH which is saturated with air is used as the liquid and pure O_2, as the gas. After a steady state of gas and liquid flow is attained, values of C_0, C_1 and C_e, are measured by a polarograph. Experimental temperature is held constant at 25±1°C. The rotational speed of the drum is changed in the range of 74~300 r.p.m. The experimental results are shown in **Table I.** **Fig. 4** shows the observed values of the thickness of the liquid film l which are calculated by Eq. (5). l increases from 0.08 to 0.2 mm at the rotating speed of 75 to 200 r.p.m. beyond which l is held approximately constant. Gas rate does not affect on the thickness of the liquid film. Comparison is made on the theoretical values of k_b calculated by Eq. (11) with the observed values calculated by Eq. (12) in **Fig. 5.** At the rotational speed greater than 115 r.p.m., both curves are in good agreement. Therefore S_n becomes nearly equal to zero and the observed data are well predicted

Table I. Absorption of O_2 into 0.1N KOH aq. solution.

Run No.	Rotating speed: N [r.p.m.]	Liquid flow rate: F_0 [cm³/sec]	$\frac{C_e-C_0}{C_e-C_i}$ [—]	l [cm]	$\frac{C_e-C_0}{C_i-C_1}$ [—]	S_n [—]	k_b exp. [cm/sec]	k_b cal. [cm/sec]
101	74	2.71	1.17	8.20×10^{-3}	0.414	−0.005	7.17×10^{-3}	8.98×10^{-3}
102	83	3.35	1.10	8.50×10^{-3}	0.385	0.00	8.20×10^{-3}	9.56×10^{-3}
103	115	6.66	1.18	1.31×10^{-2}	0.265	0.00	1.12×10^{-3}	1.13×10^{-2}
104	156	11.38	1.24	1.73×10^{-2}	0.183	0.00	1.33×10^{-3}	1.32×10^{-2}
105	212	18.90	1.15	1.95×10^{-2}	0.126	0.00	1.52×10^{-3}	1.53×10^{-2}
106	305	29.3	1.19	2.02×10^{-2}	0.0954	0.00	1.78×10^{-3}	1.84×10^{-2}

Interfacial area : $A=157$ [cm²], Molecular diffusivity of gas into liquid : $D_A=2.6\times10^{-5}$ [cm²/sec] at 25°C.

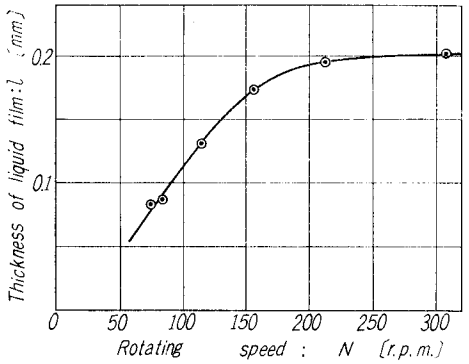

Fig. 4. Thickness of liquid film on rotating drum versus rotating speed N.

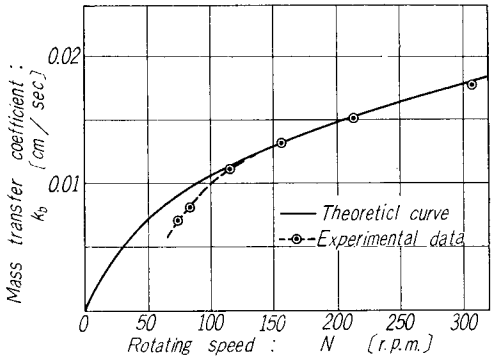

Fig. 5. Comparison of the theoretical and experimental values of k_b.

by the theoretical equation presented by Higbie, *i.e.*,

$$k_b = 2\sqrt{\frac{D_A}{\pi\tau}} = 2\sqrt{\frac{2D_AN}{\pi}} \tag{13}$$

Theoretical values of k_b are estimated by applying the published data of the diffusion coefficient of oxygen into water : $D_A=2.6\times10^{-5}$ [cm²/sec]. According to the experimental work presented by P. V. Danckwerts[3] using an analogous drum absorber, the observed values were always smaller than that of theoretical. He reported that the discrepancy may be caused by the effect of the surface resistance to diffusion. However, according to the present work there is no inconsistency, which may be caused by the liquid seal acting as a scraper (refer to **Fig. 2**). It is shown that the liquid phase mass transfer coefficient k_b varies with the rotational speed of the drum independently of the gas phase transfer coefficient k_a.

Evaporation of Water into Air (Gas Phase Mass Transfer Coefficient: k_a)

Many experimental works have been presented in gas-liquid mass transfer which showed that the over-all rate was controlled by the liquid phase mass transfer resistance. It will be interesting to estimate the resistance to diffusion in gas phase and to compare the result with that of liquid phase. In the present work the rate of evaporation of water into air is measured to give the value of k_a.

1) Mass transfer rate equation

According to E. R. Gilliland[7] diffusion coefficient in gas is very large compared with that in liquid and mass transfer may take place by steady state diffusion in the gas film.

Difference between the partial pressure of the evaporating material A at the interface p_{Ai} and the mean partial pressure of A at the cross section perpendicular to the direction of flow, p_{Aa} is taken as the driving force, then the rate of mass transfer of A per unit area of the drum surface is shown as follows:

$$N_{Ai} = k_a(p_{Ai} - p_{Aa}) \tag{14}$$

Mean transfer rate of A per unit area between the inlet and the outlet:

$$N_A = k_a \Delta p_A \tag{15}$$

where,

$$k_a = \frac{D_{Aa} P}{RT x_a p_{BM}} \tag{16}$$

Δp_A is the logarithmic mean partial pressure difference between the inlet and the outlet.

As N_A and Δp_A are easily observed, k_a is evaluated by Eq. (15) and x_a, by Eq. (16).

2) Conditions and results of experiments

Distilled water is used for circulation. Air of about 0°C is introduced and heated for use. The rate of evaporation, N_A is calculated by measuring the humidity of the air at the inlet and outlet using the dry- and wet-bulb thermometers. Experimental temperature is held at 25, 30 and 38°C. The rotational speed is in 115~285 r.p.m. and the gas flow rate is 10~65 [l/min]. A part of the experimental results is shown in **Table II.**

The logarithmic plots of the observed values of k_a in 115 r.p.m. calculated by Eq. (15) are shown by Curve (1) in **Fig. 6.** k_a is proportional to the power of 2/3 of the gas flow rate.

Table II. Vaporization of water into flowing air at atmospheric pressure, $d_e=2.4$ [cm].

Gas rate	Rotating speed	Humidity [g-water/g-dry air]		Gas temp.	Liquid temp.	N_A	d_e/x_a	k_a	$\frac{d_e\rho u_a}{\mu}$
[l/min]	[r.p.m.]	Inlet	Outlet	[°C]	[°C]	$\left[\frac{\text{g-moles}}{\text{cm}^2\cdot\text{sec}}\right]$	[—]	$\left[\frac{\text{g-moles}}{\text{cm}^2\cdot\text{sec}\cdot\text{atm}}\right]$	[—]
13.3	115	4.27×10^{-3}	1.39×10^{-2}	24.1	24.6	0.86×10^{-6}	12.6	5.68×10^{-5}	625
20.0	115	4.27×10^{-3}	1.33×10^{-2}	25.1	25.7	1.21×10^{-6}	15.1	6.78×10^{-5}	863
30.0	115	4.27×10^{-3}	1.18×10^{-2}	25.2	24.5	1.53×10^{-6}	19.6	9.12×10^{-5}	1310
39.5	115	4.27×10^{-3}	1.14×10^{-2}	25.7	25.0	1.92×10^{-6}	22.2	1.04×10^{-4}	1710
50.4	115	4.27×10^{-3}	1.03×10^{-2}	25.1	24.0	2.13×10^{-6}	27.4	1.25×10^{-4}	2230
59.0	115	4.27×10^{-3}	0.99×10^{-2}	25.5	24.0	2.38×10^{-6}	29.5	1.37×10^{-4}	2620

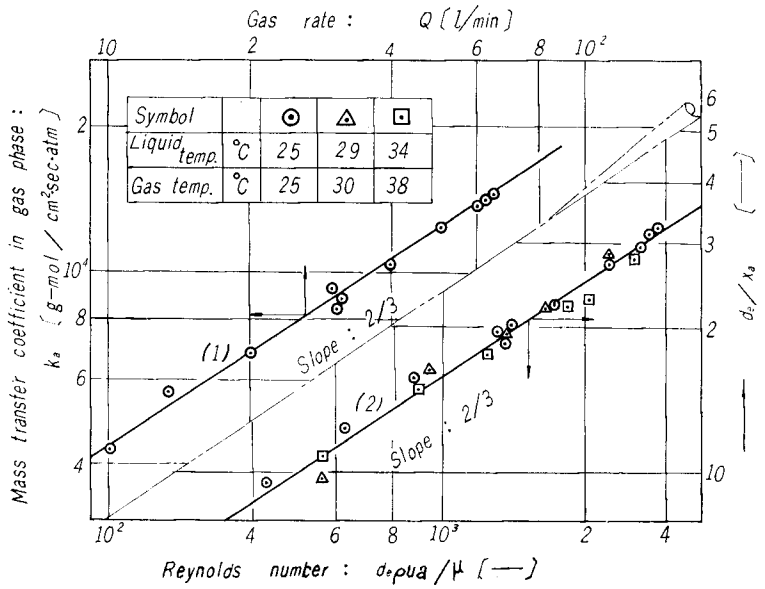

Fig. 6. k_a vs. Q and d_e/x_a vs. $d_e\rho u_a/\mu$.

When k_a is plotted against the rotational speed of the drum N, it is shown that k_a is independent of N and is a function of the gas rate only (Diagram is omitted).

Curve (2) in **Fig. 6** shows the results for different values of the diffusion coefficient of component A (D_{Aa}) and the physical properties of the gas which are changed by temperature under the same rotational speed of 115 r.p.m. The logarithmic plots of d_e/x_a versus $R_e=(d_e\rho u_a/\mu)$ are on a straight line whose slope is 2/3, hence it gives

$$\frac{d_e}{x_a}=0.164\left(\frac{d_e\rho u_a}{\mu}\right)^{2/3} \tag{17}$$

where d_e={(cross sectional area of gas stream perpendicular to the direction of flow)/(the length of the rotating drum)}×4 and u_a=absolute flow rate of the gas.

The results show that the transfer coefficient in the gas phase, k_a is changed independently of that in the liquid phase, k_b by varying the gas rate. Thickness of the effective diffusion film in the gas phase, x_a is observed. HENRY constant for O_2-H_2O system is given as 7.88×10^5 [atm/(g-moles/cc)] in Chemical Engrs' Handbook, and the observed values of $k_a=(4\sim15)\times10^{-4}$ [g-moles/cm²·sec·atm] and $k_b=(0.7\sim1.8)\times10^{-2}$ [cm/sec] in this work. Hence, Hk_a is in the range of $3.16\times10^2\sim1.18\times10^3$ [cm/sec] which are very large compared with the value of k_b.

Absorption of Oxygen into Aqueous Solution of Sodium Sulfite (Simultaneous Absorption and Chemical Reaction)

As stated above the over-all rate of reaction is affected by the rate and mechanism of the chemical reaction followed, hence they should be clarified and the rate controlling step should be determined.

The over-all rate of oxidation of sodium sulfite is changed widely in magnitude by varying the catalysts. Though the mechanism of this reaction has been studied fairly well, the rate of reaction is not yet clarified, so that the authors measure the rate precisely.

1) Liquid flow

Film theory[10], penetration theory[8], film penetration theory[16] and surface renewal theory[2], *etc.* have been presented to interpret the liquid phase resistance to diffusion of gas. In an agitation vessel and a bubble tower, *etc.* which are widely used, reaction proceeding in the bulk liquid is generally important. Hence, a test reactor which is composed of a liquid bulk and a diffusion film is useful in the application of the above theories.

Accordingly, the authors used the apparatus shown in **Fig. 7** as a schematic diagram. ① is a rotating drum which entrains a liquid film and ② is a liquid storage which is a liquid bulk. A reaction liquid contain-

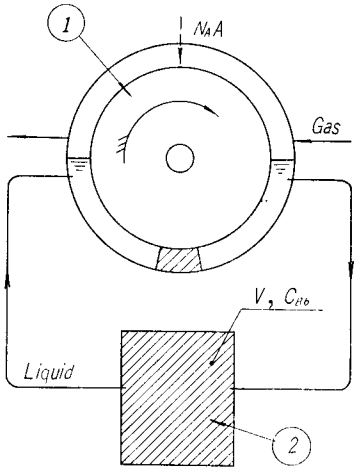

Fig. 7. Diagram showing gas-liquid contacting system consisting of a rotating liquid film and a bulk liquid.

ing a quantity of unreacted gaseous reactant may be fed into the contactor before finishing reaction in the storage ②.

The liquid phase mass transfer coefficient k_b is changed by increasing the rotating speed of the drum, and the gas phase mass transfer coefficient k_a is changed independently by the gas rate. The volume of bulk liquid per unit interfacial area $v=V/A$ is changed by increasing the liquid volume in the storage ②.

The rate of gas absorption, N_A is given by Eq. (18) by measuring the concentration of the reactant in the liquid storage ② and the time elapsed θ.

$$N_A = -\frac{V}{\nu A}\left(\frac{dC_{Bb}}{d\theta}\right) \tag{18}$$

2) Rate equation for chemical absorption

The authors presented a solution for the rate of chemical absorption in steady diffusion followed by a $(1+n)$-th order reaction for the system consisting of a liquid film and a homogeneously mixed bulk liquid in the previous paper[13]. However, the mechanism of the mass transfer in the flowing liquid in the present apparatus is unsteady and should be analysed by the penetration theory. Therefore the solution stated above may not be applicable strictly. A modification is possible, as the solutions by the film- and the penetration-theories are quite analogous in the present case.

a) Approximate solution based on film theory for $(1+n)$-th order reaction.

The following solution is obtained[13] by applying an approximate concentration distribution which is a modification of the Van Krevelen's method[17] and several numerically calculated diagrams are presented.

The solution by Van Krevelen[17] is not applicable for the system in which the concentration of the reactant gas in the bulk is not zero. For steady state diffusion occurring in the liquid film with the reaction of $(A+\nu B\rightarrow R+S)$, a basic equation is shown as follows:

$$\frac{d^2C_A}{dx^2} = \frac{1}{\nu}\frac{D_B}{D_A}\frac{d^2C_B}{dx^2} = \frac{kC_AC_B{}^n}{D_A} \tag{19}$$

The boundary conditions are

$$\left.\begin{aligned} &C_A = C_{Ai},\ \frac{dC_B}{dx} = 0 \quad \text{at} \quad x=0 \\ &-D_A\left(\frac{dC_A}{dx}\right) = kC_{Ab}C_{Bb}{}^n v \\ &C_B = C_{Bb} \end{aligned}\right\} \quad \text{at} \quad x=X_b \tag{20}$$

The concentration of the reactant A in the bulk of the phase b is given by

$$C_{Ab} = (C_A)_{x=X_b} \tag{20'}$$

An approximate solution for the rate equation: $N_A = -D_A(dC_A/dx)_{x=0}$ is as follows:

$$\frac{N_A}{k_b C_{Ai}} = \frac{Y}{\tanh Y}\left\{1-\frac{C_{Ab}}{C_{Ai}}\frac{1}{\cosh Y}\right\} \tag{21}$$

$$= \frac{1}{\kappa}\left(1-\frac{C_{Ab}}{C_{Ai}}\right) \tag{22}$$

$$Y = \gamma\left\{1-\left(\frac{1-\kappa}{\kappa}\right)\left(\frac{1}{\lambda}\right)\left(1-\frac{C_{Ab}}{C_{Ai}}\right)\right\}^{n/2} \tag{23}$$

$$\frac{C_{Ab}}{C_{Ai}} = \frac{1}{\cosh Y+(\alpha\nu)\left(\frac{\gamma}{Y}\right)\sinh Y} \tag{24}$$

where

$$\alpha = \sqrt{kC_{Bb}{}^n/D_A}\,,\quad \gamma = \sqrt{kC_{Bb}{}^n D_A}/k_b\,,\quad \kappa = X_R/X_b$$

$$(1/\lambda) = \nu\frac{D_A}{D_B}\frac{C_{Ai}}{C_{Bb}} \quad \text{and} \quad k_b = D_A/X_b$$

b) Development of the solution to unsteady state diffusion

According to the analysis by Brian[1], both plots of Hatta's[9] (film theory) and Danckwerts' solution[4] (penetration theory) for the reaction coefficient of mass transfer: $\beta^* = N_A/k_b C_{Ai}$ versus $\gamma = \sqrt{kC_{Bb}{}^n D_A}/k_b$ agree practically for the chemical absorption accompanied by a pseudo first order reaction in a system in which bulk concentration of the dissolved gas is nearly equal to zero. And also replacing the parameter λ (in β^*) for film theory by $(D_B/D_A)^{1/2}(1/\nu) \times (C_{Bb}/C_{Ai})$ in the case of fast reaction, an approximate value of β^* for penetration theory is given. The following modified solution for the Van Krevelen's equation has been derived by Brian[1] in the case of $n=1$.

$$\beta^* = \frac{N_A}{k_b C_{Ai}} = \frac{Y}{\tanh Y} \tag{25}$$

$$Y = \gamma\{1-(\beta^*-1)/(\beta_a-1)\}^{1/2} \tag{26}$$

where β_a = the value of β^* for unsteady state diffusion followed by a fast reaction. When D_B/D_A is nearly equal to unity, or β_a is large and λ is large,

$$\beta_a \fallingdotseq \sqrt{\frac{D_A}{D_B}} + \sqrt{\frac{D_B}{D_A}}\frac{1}{\nu}\frac{C_{Bb}}{C_{Ai}} \tag{27}$$

Lightfoot[11] showed that the derived solutions based on the film theory and the penetration theory agreed well in the case where the concentration of the dissolved gas in the liquid bulk was not zero and the chemical reaction was pseudo first order. From the facts, the approximate solutions derived by the authors, Eqs. (21), (22), (23) and (24) may be extended to the case where mass transfer occurs by unsteady state diffusion:

$$\beta^* = \frac{N_A}{k_b C_{Ai}} = \frac{Y}{\tanh Y}\left\{1-\frac{C_{Ab}}{C_{Ai}}\frac{1}{\cosh Y}\right\} \tag{28}$$

$$= \frac{1}{\kappa}\left(1-\frac{C_{Ab}}{C_{Ai}}\right) \tag{29}$$

$$Y = \gamma\left[1-\left\{\left(\frac{1-\kappa}{\kappa}\right)\Big/(\beta_a-1)\right\}\left\{1-\frac{C_{Ab}}{C_{Ai}}\right\}\right]^{n/2} \tag{30}$$

$$\frac{C_{Ab}}{C_{Ai}} = \frac{1}{\cosh Y+(\alpha v)\left(\frac{\gamma}{Y}\right)\sinh Y} \tag{31}$$

where

$\gamma = \sqrt{kC_{Bb}{}^n D_A}/k_b$

$k_b = 2\sqrt{D_A/\pi\tau}$

β_a = the value of β^* for unsteady state diffusion followed by a fast reaction [refer to Eq. (27)]

c) Solution for $(m+1)$-st order gas-liquid reaction.

When mass transfer occurs by steady state molecular diffusion, concentration distributions of reactants A and B are shown by Curves (1) and (1′) respectively in **Fig. 9.** A is the absorbed gas and B is the reactant in the liquid phase. The reaction in liquid is,

$$A+\nu B \rightarrow R+S \tag{32}$$

and the order of reaction with the concentrations of A and B are m and unity respectively. Taking the material balance in the differential volume between two surfaces at a distance x and $x+dx$ from the interface, we have

$$\frac{d^2C_A}{dx^2} = \frac{1}{\nu}\frac{D_B}{D_A}\frac{d^2C_B}{dx^2} = \frac{kC_A{}^mC_B}{D_A} \tag{33}$$

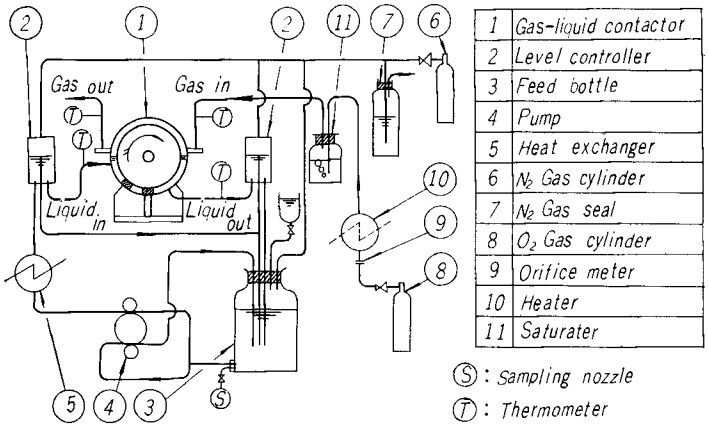

Fig. 8. Flow sheet for absorption of O_2 into 0.1 N Na_2SO_3 aq. solution with a rotating drum gas-liquid contactor.

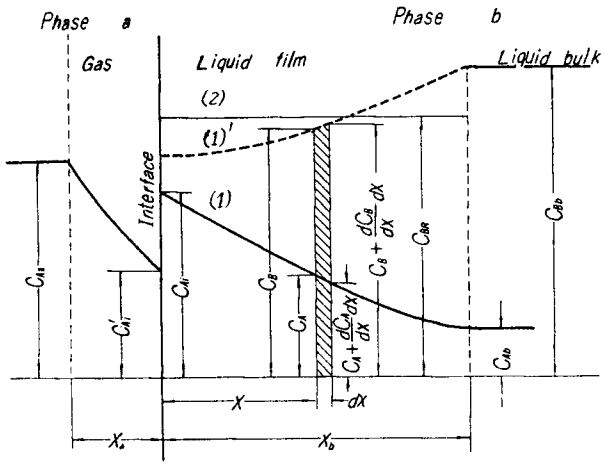

Fig. 9. Concentration distribution of reactants in the vicinity of interface when $C_B=C_{BR}$=constant.

Assuming that $C_B=C_{BR}$ (=const.)$\leqq C_{Bb}$ in the liquid film as shown by Curve (2) in **Fig. 9,** Eq. (33) is rewritten as:

$$\frac{d^2C_A}{dx^2}=\frac{kC_{BR}}{D_A}C_A{}^m \tag{34}$$

The value $2dC_A/dx$ is multiplied to both side terms of Eq. (34), we have the following equation which shows the concentration distribution within the diffusion film.

$$-\frac{dC_A}{dx}=\frac{C_{Ai}}{x_b}\sqrt{Y^2\left(\frac{C_A}{C_{Ai}}\right)^{m+1}+K} \tag{35}$$

where K is an integration constant, and

$$Y=\alpha x_b=\sqrt{\left(\frac{2}{m+1}\right)kC_{Ai}{}^{m-1}C_{BR}D_A}\Big/k_b \tag{36}\dagger$$

$$\alpha=\sqrt{\left(\frac{2}{m+1}\right)\frac{kC_{Ai}{}^{m-1}C_{BR}}{D_A}} \tag{37}\dagger$$

$$k_b=D_A/x_b \tag{38}$$

The boundary conditions are

$$\left.\begin{aligned}C_A&=C_{Ai} \quad \text{at} \quad x=0\\ C_A&=C_{Ab} \quad \text{at} \quad x=x_b\end{aligned}\right\} \tag{39}$$

The rate of reaction per unit interfacial area, N_A is obtained from Eqs. (35)

† When $m=1$, $Y=\sqrt{kC_{BR}D_A}/k_b$, $\alpha=\sqrt{kC_{BR}/D_A}$.
These results agree with the solution presented in the previous paper[13].

and (39) as follows:

$$N_A = -D_A\left(\frac{dC_A}{dx}\right)_{x=0} = D_A\frac{C_{Ai}}{x_b}\sqrt{Y^2+K}$$
$$= k_b C_{Ai}\sqrt{Y^2+K} \tag{40}$$

Hence, the reaction coefficient for mass transfer, β^* is written as follows:

$$\beta^* = \frac{N_A}{k_b C_{Ai}} = \sqrt{Y^2+K} \tag{41}$$

The equation to give the integration constant is derived from Eq. (35).

$$-\int_{\frac{C_{Ab}}{C_{Ai}}}^{1}\frac{(dC_A/C_{Ai})}{\sqrt{Y^2\left(\frac{C_A}{C_{Ai}}\right)^{m+1}+K}} = \frac{1}{x_b}\int dx \tag{42}$$

Eq. (42) is solved with the boundary conditions of Eq. (39).
We have for $m=0$,

$$K = \left(\frac{C_{Ab}}{C_{Ai}}\right)^2 - 2\left(\frac{C_{Ab}}{C_{Ai}}\right)\left(1+\frac{Y^2}{4}\right) + \left(1-\frac{Y^2}{4}\right)^2 \tag{43}$$

Similarly for $m=1$,

$$K = 4e^Y\frac{Y^2}{(e^{2Y}-1)^2}\left[\frac{C_{Bb}}{C_{Ai}}\left\{\frac{C_{Ab}}{C_{Ai}}e^Y - e^{2Y} - 1\right\} + e^Y\right] \tag{44}$$

From Eqs. (43) and (44), the value of K for $m=0$ and unity is given by taking C_{Ab}/C_{Ai} as a parameter for various values of Y.

For the general case where m is neither zero nor unity, Eq. (42) is rewritten with the conditions of Eq. (39) as follows:

$$-\int_{\frac{C_{Ab}}{C_{Ai}}}^{1}\frac{d(C_A/C_{Ai})}{\sqrt{Y^2\left(\frac{C_A}{C_{Ai}}\right)^{m+1}+K}} = 1 \tag{45}$$

Although analytical solutions of Eq. (45) may not be obtainable, the relation between K and Y is given by a numerical calculation.

d) Numerically calculated diagram of β^* versus γ for reaction of $(m+1)$-st order.

By preparing a supplemental diagram of β^* versus Y in which C_{Ab}/C_{Ai} is used as a parameter, diagrams of β^* versus γ in the previous paper[13] for (1+1)-st order reaction are also useful for the $(m+1)$-st order reaction as mentioned below.

The value of β^* for a specified value of Y is calculated from Eq. (41), by taking C_{Ab}/C_{Ai} as the parameter, using Eq. (43) for $m=0$ and Eq. (44) for $m=1$ and is plotted against Y on **Fig. 10.** Similarly for other values of m, the relation between β^* versus Y is given by Eq. (41) introducing the relation between K and Y which is given by numerical calculation.

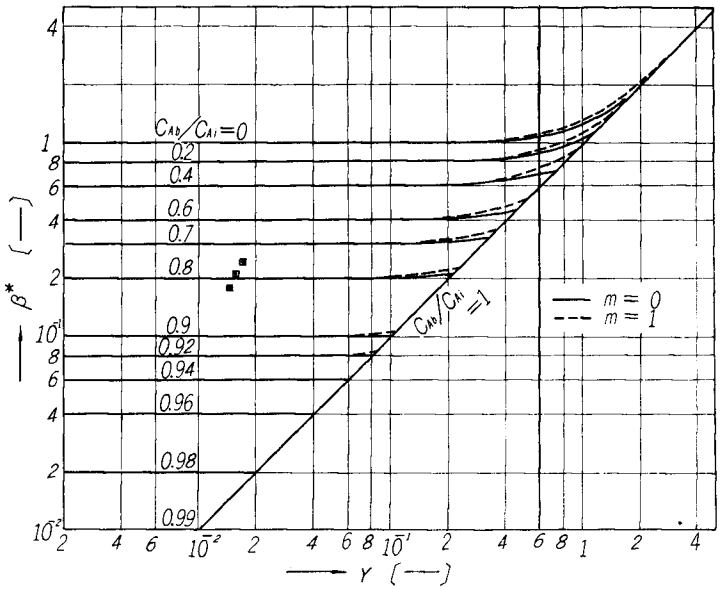

Fig. 10. β^* vs. Y for $m=0$ and 1 where C_{Ab}/C_{Ai} is taken as the parameter.

e) Application procedure of the diagram of β^* versus γ.

In the case where $C_{BR}\fallingdotseq C_{Bb}$, that is, $Y\fallingdotseq\gamma$, Y is calculated by Eq. (36) by substituting the observed values of C_{Bb}, m, k, k_b, C_{Ai} and D_A, and the value of β^* is calculated from Eq. (41) by introducing the experimental values of N_A, k_b and C_{Ai}.

The value of C_{Ab}/C_{Ai} corresponding to these values of Y and β^* are read on the curves in **Fig. 10.** Then, the value of αv is calculated from Eq. (46) which was presented in the previous paper[13] by introducing C_{Ab}/C_{Ai} and Y thus obtained,

$$\frac{C_{Ab}}{C_{Ai}}=\frac{1}{\cosh Y+(\alpha v)\left(\frac{\gamma}{Y}\right)\sinh Y} \tag{46}$$

The β^* versus γ diagrams presented in the previous paper[13] are applicable, when the values of Y, β^* and αv are given by the procedure mentioned above.

3) Rate controlling steps and rate equations in chemical absorption

The following five steps of rate controlling are postulated by the approximate solution, Eqs. (21), (22), (23) and (24), and also by the approximate rate equations (28), (29), (30) and (31).

a) Chemical reaction resistance controlling

This is the case where γ and $\gamma(\alpha v)$ are very small and the rate of absorption, N_A is expressed approximately by Eq. (47).

$$N_A = kC_{Ai}C_{Bb}{}^n v \tag{47}$$

When the over-all rate is proportional to $C_{Ai}{}^m$, Eq. (47) is written as follows:

$$N_A = kC_{Ai}{}^m C_{Bb}{}^n v \tag{48}$$

In the case of $n=1$, the rate equation for the reaction of Eq. (32) is written as follows:

$$-\frac{1}{\nu}\frac{dC_{Bb}}{d\theta} = kC_{Ai}{}^m C_{Bb} \tag{48'}$$

Eq. (48') is integrated into the following form.

$$\ln(C_{Bb}/C_{Bbo}) = -\nu k C_{Ai}{}^m \theta \tag{49}$$

where C_{Bbo} is the value of C_{Bb} at $\theta=0$.

Hence, the observed data of C_{Bb} and C_{Bbo} corresponding to more than two values of C_{Ai} for the same time θ, that is, C_{Bb} and C_{Bbo} as well as C_{Bb}' and C_{Bbo}', are introduced into Eq. (49). Taking the ratio of these two equations, we have:

$$\left(\frac{C_{Ai}}{C_{Ai}'}\right)^m = \frac{\ln(C_{Bb}/C_{Bbo})}{\ln(C_{Bb}'/C_{Bbo}')} \tag{50}$$

The value of m is determined by Eq. (50). The reaction rate constant is calculated by the relation.

$$k = -\frac{\ln(C_{Bb}/C_{Bbo})}{\nu C_{Ai}{}^m \theta} \tag{51}$$

b) Both diffusion and reaction resistances controlling

This is the case where (αv) is large and $\gamma(\alpha v)$ is not negligible compared with unity for small value of γ.

Approximate rate equation is shown as follows:

$$N_A = \frac{C_{Ai}}{1/k_b + 1/kC_{Bb}{}^n v} \tag{52}$$

For the other cases except $\gamma \ll 1$, general equations (28)~(31) should be applied.

c) Diffusion resistance of dissolved gaseous reactant controlling

When γ is small and (αv) is very large, an approximate rate equation is obtained as follows:

$$N_A = k_b C_{Ai} \tag{53}$$

d) Diffusion resistance and reaction resistance within liquid diffusion film controlling

When $\gamma>4$ and C_{Bb}/C_{Ai} is very large, approximate rate equation is derived as follows:

$$N_A = k_b C_{Ai}\gamma = \sqrt{kC_{Bb}^n D_A}\cdot C_{Ai} \tag{54}$$

e) Diffusion resistance of a reactant from liquid bulk controlling

When γ is very large, approximate rate equation is derived as follows:

$$N_A = k_b C_{Ai}\left\{1+\frac{1}{\nu}\left(\frac{D_B}{D_A}\right)\left(\frac{C_{Bb}}{C_{Ai}}\right)\right\} \tag{55}$$

(film theory)

$$N_A = k_b C_{Ai}\left\{\sqrt{\frac{D_A}{D_B}}+\frac{1}{\nu}\sqrt{\frac{D_B}{D_A}}\frac{C_{Bb}}{C_{Ai}}\right\} \tag{56}$$

(penetration theory)

where $k_b=D_A/X_b$ in Eq. (55) and $k_b=2\sqrt{D_A/\pi\tau}$ in Eq. (56).

4) Determination of rate controlling step using a gas-liquid contactor of rotating drum type

According to Eqs. (47), (52), (53), (54) and (56), the rate controlling steps are classified as follows.

A. Diffusion resistance in liquid phase controlling: The rate of absorption is not changed by the flow rate of gas.

(1) Reaction resistance controlling: Over-all rate is proportional to the liquid volume per unit interfacial area (v) and is independent of k_b or rotational speed of the drum, N.

(2) Diffusion and reaction resistances controlling: Over-all rate is changed by both v and N.

(3) Diffusion resistance of dissolved gas controlling: Over-all rate is changed by N and is independent of v. The concentration of the reactant in the liquid phase is nearly equal to zero ($C_{Ab}\fallingdotseq 0$).

(4) Diffusion and reaction resistances within liquid diffusion film controlling: Over-all rate is changed by C_{Bb} ($C_{Ab}\fallingdotseq 0$) and is independent of both N and v.

(5) Diffusion resistance of reactant from liquid bulk, controlling: Over-all rate is greater than that for the case (3) and is changed by N and C_{Bb} ($C_{Ab}\fallingdotseq 0$).

B. Resistance in gas phase controlling

The rate of absorption is changed only by the flow rate of gas.

5) Chemical reaction

Over-all oxidation reaction of sodium sulfite with oxygen is shown as

follows:

$$O_2 + 2Na_2SO_3 \rightarrow 2Na_2SO_4 \tag{57}$$

The rate of chemical reaction increases with addition of Cu or Co ion as the catalysts and decreases with *d*-mannitol ($C_6H_{14}O_6$) or ethyl alcohol as the negative catalysts[5].

6) Measuring methods

Fig. 8 is the flow sheet of the experiment. Before liquid is charged, air in the whole apparatus is displaced by N_2 gas from the gas holder ⑥.

0.1 N sodium sulfite aqueous solution is used as the reaction liquid. Gaseous reactants O_2 and air are introduced after a steady state of liquid flow is attained. Liquid sample is taken from the reaction bottle ③ and the concentration of unreacted sodium sulfite and the time elapsed are measured. A liquid sample of 10 cc is mixed with aqueous solution of KI containing HCl and the residual concentration of Na_2SO_3 is titrated by aqueous solution of KIO_3 using starch as an indicator. Rate of absorption is calculated by Eq. (18).

Reaction temperature is held constant at 25±1°C in both liquid and gas. Experimentation is performed at the rotational speed of the drum in 115, 200 and 285 r.p.m. Agitator speed is held constant at 750 r.p.m. in the case of experiments performed in an agitation vessel.

7) Results and Discussion

a) A case of reaction resistance controlling (Negative catalyst: *d*-mannitol)

Curves (1), (2) and (3) in **Fig. 11** show the observed data of oxidation of sodium sulfite aqueous solution which contains chemically pure *d*-mannitol in concentration of 10^{-1} [g-moles/*l*] with pure oxygen. The volume of liquid is 800 cc.

Concentration change in the parts (A) of Curves (1), (2) and (3) in **Fig. 11,** *i.e.*, the parts at which C_{Bb} is less than 6×10^{-3} [g-moles/*l*], are replotted as shown on the top of the right hand side in **Fig. 11.** The rate of absorption is not changed by the rotational speed of the drum.

Curves (4) and (5) in **Fig. 11** show the results of oxidation of Na_2SO_3 aqueous solution containing recrystallized pure *d*-mannitol as the negative catalyst in concentration of 5×10^{-4} [g-moles/*l*]. Curves (6) and (7) show the data for the same condition using ethyl alcohol as the catalyst in concentration of 4.33×10^{-4} [g-moles/*l*].

Plots of these results on a semi-logarithmic paper give a straight line.

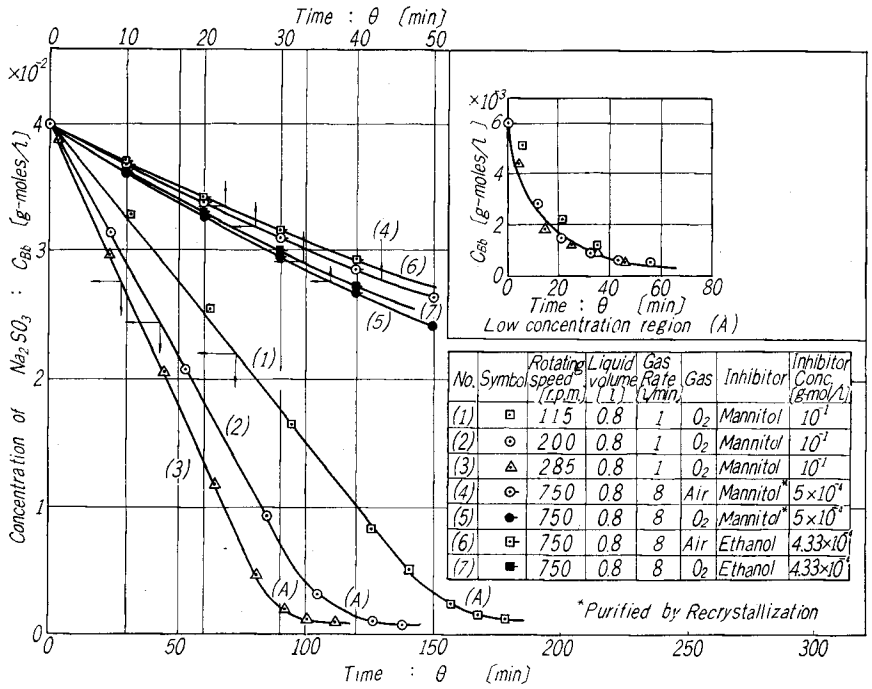

No.	Symbol	Rotating speed (r.p.m.)	Liquid volume (l)	Gas Rate (l/min)	Gas	Inhibitor	Inhibitor Conc. (g-mol/l)
(1)	□	115	0.8	1	O_2	Mannitol	10^{-1}
(2)	⊙	200	0.8	1	O_2	Mannitol	10^{-1}
(3)	△	285	0.8	1	O_2	Mannitol	10^{-1}
(4)	⊙	750	0.8	8	Air	Mannitol*	5×10^{-4}
(5)	●	750	0.8	8	O_2	Mannitol*	5×10^{-4}
(6)	⊞	750	0.8	8	Air	Ethanol	4.33×10^{-1}
(7)	■	750	0.8	8	O_2	Ethanol	4.33×10^{-1}

Fig. 11. Oxidation of sodium sulfite; *d*-Mannitol used as the inhibiter.

The over-all rate is proportional to the first order of the concentration of Na_2SO_3.

Interface concentration of oxygen in the liquid phase for O_2–H_2O system, (C_{Ai}) and that for air–H_2O system (C_{Ai}') are as follows:

$$C_{Ai} = 1.23\times10^{-3}\ [\text{g-moles}/l] \tag{58}$$

$$C_{Ai}' = 2.36\times10^{-4}\ [\text{g-moles}/l] \tag{59}$$

Therefore,

$$(C_{Ai}/C_{Ai}') = 5.20 \tag{60}$$

In the case of mannitol, the data of Curves (4) and (5) in **Fig. 11** at time $\theta=40$ min are substituted into Eq. (50), then we have,

$$(5.2)^m = \frac{\ln(2.68\times10^{-2}/4.00\times10^{-2})}{\ln(2.86\times10^{-2}/4.00\times10^{-2})} = 1.190 \tag{61}$$

From Eq. (61), $m=0.1055$.

Similarly for the negative catalyst of ethyl alcohol, Curves (6) and (7) are obtained and we have $m=0.1050$. Taking the mean values of m we have for m

$$m = 0.105 \tag{62}$$

Because ν is equal to 2 in Eq. (49) (refer to Eq. (57)) the reaction rate constant is determined as follows:

$$k = -\left\{\ln\left(\frac{C_{Bb}}{C_{Bbo}}\right)\right\}\Big/ 2C_{Ai}{}^{m}\theta \tag{63}$$

From the data for mannitol and pure O_2 (refer to Curve (5) in **Fig. 11**), C_{Bbo} is equal to 4.00×10^{-2} and C_{Bb} at 40 min is equal to 2.68×10^{-2} [g-moles/l], and the value of k is determined as follows:

$$k = 1.68\times10^{-4}\ [(l/\text{g-moles})^{0.105}/\text{sec}] \tag{64}$$

$$= 3.47\times10^{-4}\ [(\text{cm}^3/\text{g-moles})^{0.105}/\text{sec}] \tag{64'}$$

b) Diffusion and reaction resistance controlling

For the range of concentration $C_{Bb}\geqq6\times10^{-3}$ [g-moles/l] holding other reaction conditions the same, the rate of absorption is increased by increasing the rotational speed of the drum as shown by Curves (1), (2) and (3) in **Fig. 11.** Effect of change in N for the value of k_b is apparent as shown by Eq. (13).

c) Diffusion resistance of dissolved gas controlling (Pure O_2 absorption in liquid containing no catalyst)

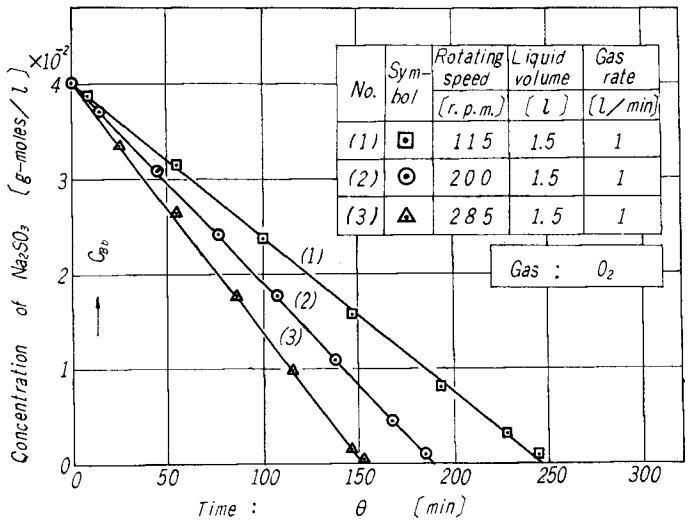

Fig. 12. C_{Bb} vs. θ for oxidation of sodium sulfite without catalyst.

Fig. 12 shows the results of oxidation of Na_2SO_3-solution of 1500 cc with pure oxygen. The curves are linear regardless of the rotational speed of the drum though the slope is different. The relation between N_A and β^* is shown as follows:

$$\beta^* = N_A/k_bC_{Ai} \fallingdotseq 1 \tag{65}$$

which agrees with Eq. (53). This is the case of diffusion resistance controlling and the rate is equal to that of physical absorption where the concentration of the dissolved gas in the bulk liquid is zero. In this stage, the reaction rate constant k is not determined. Hence, published data by other author[15] is adopted.

d) Resistances to diffusion and chemical reaction within the diffusion film of liquid controlling (Catalyst: $CoSO_4$, Gas: Air)

Fig. 13 shows the results of oxidation of Na_2SO_3 solution of 1500 cc containing $CoSO_4$ of 5×10^{-4} [g-moles/l] as the catalyst with air. Difference in

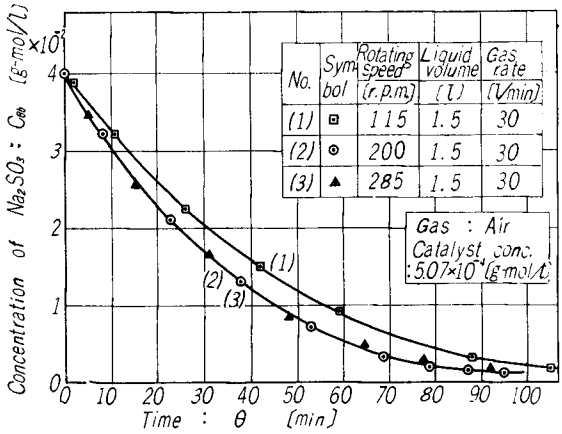

Fig. 13. C_{Bb} vs. θ for oxidation of sodium sulfite with catalyst of $CoSO_4$.

rate, N_A, is not observed with change in rotational speeds from 200 to 285 r.p.m.. Also the difference between 200 and 115 r.p.m. is very small. Hence, this is the case of both resistances controlling in the diffusion film. From Eqs. (18) and (54), the following approximate rate equation holds for 1st order with C_{Ai} and n-th order with C_{Bb}.

$$\frac{1}{2}\frac{v}{C_{Ai}}\left(-\frac{dC_{Bb}}{d\theta}\right) = \sqrt{kD_A}\cdot C_{Bb}^{n/2} \tag{66}$$

Plots of $(1/2)(v/C_{Ai})(-dC_{Bb}/d\theta)$ versus C_{Bb} on a log-log paper gives a straight line of slope 3/4 for the rotational speed of 285 and 200 r.p.m. as shown in **Fig. 14.** From the slope, the order of reaction with C_{Bb} is determined to be:

$$n = 3/2 \tag{67}$$

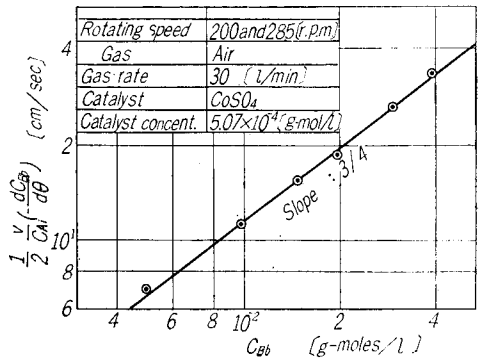

Fig. 14. $\frac{1}{2}\frac{v}{C_{Ai}}\left(-\frac{dC_{Bb}}{d\theta}\right)$ vs. C_{Bb}.

e) Diffusion resistance of reactant in liquid bulk controlling
(Catalyst: $CoSO_4$, Gas: pure O_2)

Fig. 15 shows the results of oxidation of the same liquid of 2500 cc as used in the experiments stated in **d**) with pure O_2. Though the value of C_{Ai} is increased 4.76 times as large compared with the value shown in **Fig. 13,** the rate of absorption is not increased so much. The rate of absorption is clearly changed by the rotational speed of the drum. This may be an evidence of diffusion resistance controlling of the reactant (Na_2SO_3) in the liquid.

Fig. 16 shows the plots of the observed values of β^* versus γ, on the theoretical curves which are drawn by Eqs. (28) to (31) for $\alpha v=\infty$ and $n=1.5$ (cases (**e**) and (**d**)). From this diagram the value of k is determined to be,

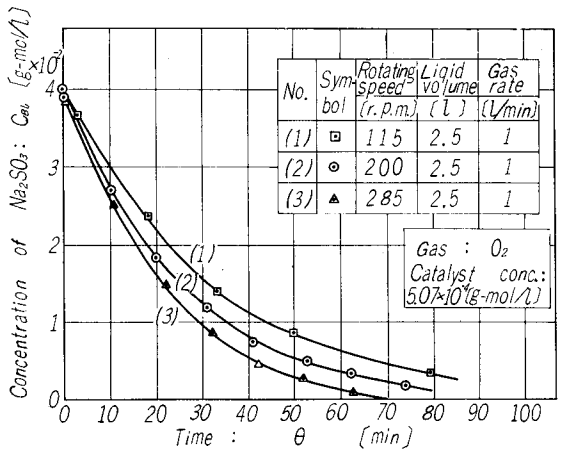

Fig. 15. Oxidation of sodium sulfite with catalyst of $CoSO_4$.

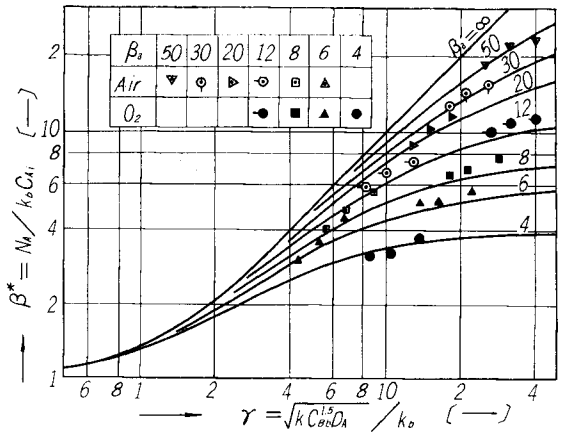

Fig. 16. Comparison of experimental results with theoretical curve of β^* vs. γ.

$$k = 1.03\times10^6\ (l/\text{g-mole})^{1.5}\,(1/\text{sec}) \tag{68}$$

That the rate of reaction catalyzed by $CoSO_4$ is proportional to first order of C_{Ai}, *i.e.*, $m=1$ and Eqs. (66) and (68) are applicable, is verified, because as shown in **Fig. 16** the data for air and O_2 of the same value of β_a fall on the same curve when β^* and γ are plotted using k from Eq. (68).

f) Effect of diffusion resistance in gas film

When air is used as the gaseous reactant in the experiment, **d)**, the resistance in the gas film may be pertaining.

Fig. 17 shows the observed results when the liquid flow condition is the

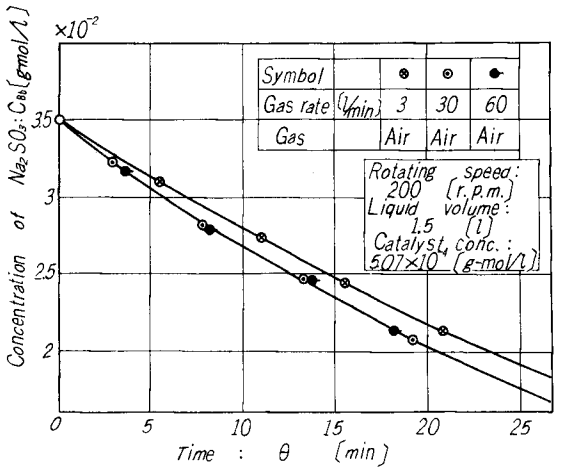

Fig. 17. C_{Bb} vs. θ curves for oxidation of sodium sulfite showing the effect of gas film resistance.

same as that in **d**), *i.e.*, the rotational speed, $N=200$ r.p.m.. Although the gas flow rate is changed, the rate of absorption is equal in the cases of air flow rate of 30 and 60 [l/min]. The effect of air rate begins to appear when gas rate is lowered to 3 [l/min]. Hence, the resistance in the gas phase is negligible in the experimental conditions mentioned in **d**).

g) Effect of catalyst

Fig. 18 shows the plots of the observed values of (C_{Bb}/C_{Bbo}) versus $(\nu k_b C_{Ai}\theta/vC_{Bbo})$ in $N=200$ r.p.m. in order to compare the effect of the various catalysts. The value of β^* is given by the slope of the curves in **Fig. 18.**

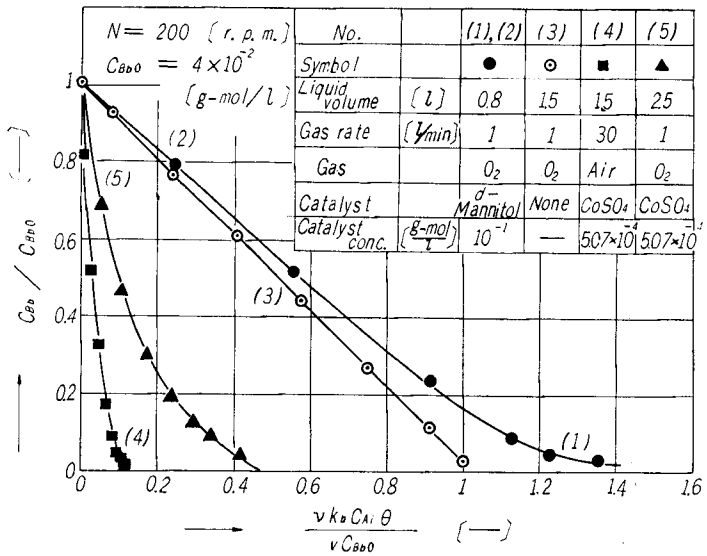

Fig. 18. Effect of catalyst on rate of absorption.

h) β^* versus γ

In the case of reaction rate controlling shown in Curves (4) to (7) in **Fig. 11** where purified *d*-mannitol is used as the negative catalyst, Y is nearly equal to γ and Eq. (46) is simplified to

$$\frac{C_{Ab}}{C_{Ai}}=\frac{1}{\cosh Y+(\alpha v)\sinh Y} \tag{69}$$

As $\cosh Y\fallingdotseq 1$ and $\sinh Y\fallingdotseq Y$, when Y is small, αv is calculated by the equation:

$$\alpha v=\frac{1-(C_{Ab}/C_{Ai})}{Y(C_{Ab}/C_{Ai})} \tag{70}$$

Substituting the data : $m=0.105$, $D_A=2.60\times10^{-5}$ [cm^2/sec], $v=1.91$ [cm^3/cm^2] ($V=300$ cc), $k_b=2.10\times10^{-2}$ [cm/sec] ($N=400$ r.p.m.) and $k=1.68\times10^{-4}$ [(l/g-moles)$^{0.105}$

/sec] (Eq. (64)) into Eqs. (36), (41) and (48′), these values of the related parameter for several values of C_{Bb} in oxidation by pure oxygen are calculated and tabulated in **Table III.**

Table III. Na_2SO_3–O_2 system with negative catalyst of purified *d*-mannitol.

$C_{Bb}\times10^5$	$R\times10^9$	$Y\times10^2$	β^*	$C_{Ab}C/_{Ai}$	αv	αv^*
[g-moles/cm³]	[g-moles/cm³·sec]	[—]	[—]	[—]	[—]	[—]
3.96	3.29	1.70	0.243	0.757	18.8	26.2
3.41	2.84	1.58	0.210	0.790	16.8	24.2
2.91	2.42	1.45	0.179	0.821	15.0	22.4

* Calculated from Eq. (37) and the specified values of v.

The last column in **Table III** shows the value of αv which is given by the value of α calculated by Eq. (37) and v specified by the experimental condition. These values of αv do not coincide with those calculated by Eq. (70). As $Y \fallingdotseq \gamma$ in this case, values shown in **Table IV** are plotted on **Fig. 19.** It is seen that the result shown in **Table III** is the case of reaction rate controlling.

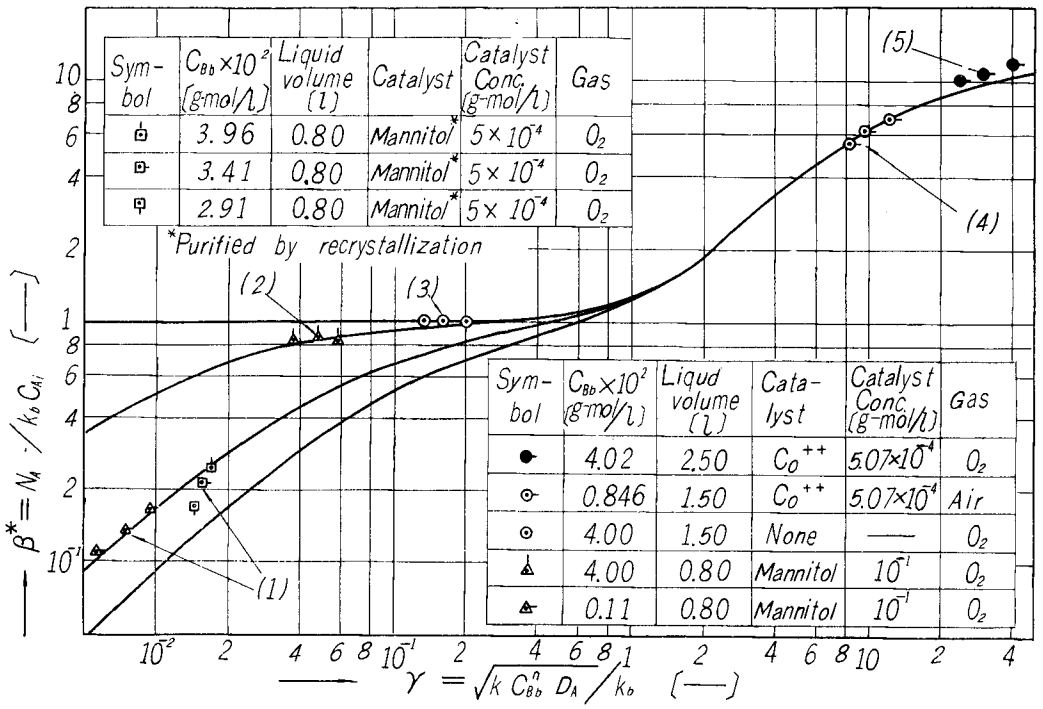

Fig. 19. β^* vs. γ, comparison of experimental results with theory.

Table IV. Oxidation of sodium sulfite.

Rotating speed	Liquid volume	Catalyst	Catalyst concent.	k	n
[r.p.m.]	[l]		[g-moles/l]	$(l/\text{g-moles})^n \frac{1}{\text{sec}}$	[—]
115	0.8	*d*-Mannitol	10^{-1}	0.367	1
200	0.8	*d*-Mannitol	10^{-1}	0.367	1
285	0.8	*d*-Mannitol	10^{-1}	0.367	1
115	0.8	*d*-Mannitol	10^{-1}	0.367	1
200	0.8	*d*-Mannitol	10^{-1}	0.367	1
285	0.8	*d*-Mannitol	10^{-1}	0.367	1
115	1.5	None	—	(5.6)[15]	1
200	1.5	None	—	(5.6)	1
285	1.5	None	—	(5.6)	1
115	1.5	$CoSO_4$	5×10^{-4}	1.03×10^{6}	1.5
200	1.5	$CoSO_4$	5×10^{-4}	1.03×10^{6}	1.5
285	1.5	$CoSO_4$	5×10^{-4}	1.03×10^{6}	1.5
115	2.5	$CoSO_4$	5×10^{-4}	1.03×10^{6}	1.5
200	2.5	$CoSO_4$	5×10^{-4}	1.03×10^{6}	1.5
285	2.5	$CoSO_4$	5×10^{-4}	1.03×10^{6}	1.5

Rotating speed	C_{Bb}	k_b	γ obs.	β^* obs.	Gas
[r.p.m.]	[g-moles/l]	[cm/sec]	[—]	[—]	
115	0.11×10^{-2}	1.13×10^{-2}	9.05×10^{-3}	1.82×10^{-1}	O_2
200	0.11×10^{-2}	1.49×10^{-2}	6.9×10^{-3}	1.37×10^{-1}	O_2
285	0.11×10^{-2}	1.77×10^{-2}	5.8×10^{-3}	1.14×10^{-1}	O_2
115	4.0×10^{-2}	1.13×10^{-2}	5.5×10^{-2}	7.65×10^{-1}	O_2
200	4.0×10^{-2}	1.49×10^{-2}	4.16×10^{-2}	8.55×10^{-1}	O_2
285	4.0×10^{-2}	1.77×10^{-2}	3.49×10^{-2}	8.45×10^{-1}	O_2
115	4.0×10^{-2}	1.13×10^{-2}	(2.14×10^{-1})	0.98	O_2
200	4.0×10^{-2}	1.49×10^{-2}	(1.63×10^{-1})	0.98	O_2
285	4.0×10^{-2}	1.77×10^{-2}	(1.37×10^{-1})	1.01	O_2
115	8.46×10^{-3}	1.13×10^{-2}	12.8	7.70	Air
200	8.46×10^{-3}	1.49×10^{-2}	9.82	6.95	Air
285	8.46×10^{-3}	1.77×10^{-2}	8.22	5.75	Air
115	4.02×10^{-2}	1.13×10^{-2}	40.9	12.1	O_2
200	4.02×10^{-2}	1.49×10^{-2}	31.5	10.9	O_2
285	4.02×10^{-2}	1.77×10^{-2}	26.3	10.2	O_2

Temperature: 25±1°C at atmospheric pressure.

The values of β^* and γ calculated from the experimental results shown in the paragraph **a**) (which are obtained by the experiment of uncrystallized *d*-mannitol), **b**), **c**), **d**) and **e**) are tabulated in **Table IV.** Observed values and the theoretical curves of Eqs. (28), (29), (30) and (31) are plotted on the same diagram, **Fig. 19.**

Group (1) of the plotted points in **Fig. 19** are in the range of chemical reaction rate controlling; group (2), diffusion and chemical reaction rate controlling; group (3), diffusion rate of reactant A controlling; group (4), diffusion and chemical reaction rate controlling within the diffusion film; and group (5), diffusion rate of reactant B from the liquid bulk controlling. The theoretical and experimental values are in good agreement. Hence, approximate solution presented by the authors based on the film theory may be extended to the case of unsteady state mass transfer which should be rightfully predicted by the penetration theory. From this plots, the rate controlling steps are clearly shown and the change in β^* with increase in γ is evident.

Conclusions

A gas-liquid contactor of a rotating drum was contrived as a test reactor in which the interfacial area between phases was measurable.

The rate of oxidation of sodium sulfite with O_2 and air was observed in the system consisting of a liquid film and a separate bulk liquid. The rate and the order of reaction were measured. Solution for the rate equation of $(m+1)$-st order was also derived as the supplement for the previous paper[13]. The observed results were plotted on the theoretical curves and comparison were made. The existence of five states of rate controlling effected by the relative magnitude of reaction and diffusion resistances, which were derived by theoretical analysis, were verified by experiment.

Acknowledgment

The authors express their thanks to Mr. N. Hashimoto, K. Watanabe and F. Murakami for the co-operation in these studies.

Notations Used

A : Total interfacial area [cm²]
A : Reactant A (gas) [—]
B : Reactant B (liquid) [—]
B : Width of rotating cylinder [cm]
C, C_0, C_1 and C_e: Concentration of dissolved gas in liquid (refer to **Figs. 2 and 3**) [g-mol/l]
C_A : Concentration of reactant A in liquid [g-mol/l]
C_{Ab} : Uniform bulk liquid concentration of A [g-mol/l]
C_{Ai} : Concentration of reactant A in liquid at gas-liquid interface [g-mol/l]
C_B : Concentration of reactant B in liquid [g-mol/l]
C_{Bb} : Uniform bulk liquid concentration of B [g-mol/l]
B_{Bbo}: C_{Bb} at time $\theta=0$ [g-mol/l]
C_{BR} : Average concentration of reactant B (assumed) in reaction zone of liquid phase [g-mol/l]
C_i : Concentration of dissolved gas (A) in liquid at interface [g-mol/l]
D_A : Molecular diffusivity of reactant A in liquid [cm²/sec]
D_{Aa} : Molecular diffusivity of reactant A in phase a [cm²/sec]
D_B : Molecular diffusivity of reactant B in liquid [cm²/sec]
d : Diameter of rotating drum [cm]
d_e : Equivalent diameter of gas stream [cm]
F, F_0, ΔF: Liquid flow rate (refer to **Fig. 2**) [cm³/sec]
H : HENRY constant [atm/(g-mol/cc)]
k : Reaction rate constant for $(1+n)$-th order reaction [$(l$/g-mol$)^n$/sec]
k : Reaction rate constant for $(m+1)$-st order reaction [$(l$/g-mol$)^m$/sec]
k_a : Gas film mass transfer coefficient [g-mol/cm²·sec·atm]
k_b : Liquid-phase mass transfer coefficient (in absence of chemical reaction) [cm/sec]
K : Integration constant [—]
l : Thickness of liquid film on rotating cylinder [cm]
m : Order of reaction (on C_A) [—]
n : Order of reaction (on C_{Bb}) [—]
N : Rotating speed of drum [r.p.m.] or [r.p.s.]
N_A : Average rate of absorption or evaporation per unit area of interface [g-mol/cm²]
N_{Ai} : Rate of vaporization per unit area of interface [g-mol/cm²]
p_{Aa} : Mean partial pressure of diffusing gas in gas stream [atm]
p_{Ai} : Partial pressure of diffusing gas at phase boundary [atm]

Δp_A : Mean difference between vapor pressure of liquid and partial pressure in gas stream [atm]
p_{BM} : Logarithmic mean partial pressure of inert gas through which vapor diffuses [atm]
P : Total pressure [atm]
R : Gas constant [cm³·atm/g-mol·°K]
t : Time [sec]
u_a : Absolute velocity of gas [cm/sec]
v : Liquid volume per unit interfacial area [cm]
V : Liquid volume [cm³]
x : Distance normal to the interface [cm]
X_a : Thickness of effective gas film [cm]
X_b : Thickness of liquid film [cm]
X_R : Thickness of effective reaction zone in liquid phase[13] [cm]
$Y=\sqrt{kC_{BR}{}^nD_A}/k_b$: Parameter for $(1+n)$-th order reaction [—]
$\alpha=\sqrt{kC_{Bb}{}^n/D_A}$: Parameter for $(1+n)$-th order reaction [1/cm]
$\beta^*=N_A/k_bC_{Ai}$: Reaction coefficient for mass transfer [—]
β_a : β^* for unsteady state diffusion followed by fast irreversible reaction [—]
$\gamma=\sqrt{kC_{Bb}{}^nD_A}/k_b$: Parameter for $(1+n)$-th order reaction [—]
θ : Time [sec]
$\kappa=X_R/X_b$ [—]
λ : $(1/\nu)(D_B/D_A)(C_{Bb}/C_{Ai})$ [—]
μ : Viscosity [g/cm·sec]
ν : Number of moles of B reacting with one mole of A [—]
ρ : Density [g/cm³]
τ : Gas-liquid contact time [sec]

Literature cited

1) Brian, P. L. T., *Sc. Thesis in Chemical Engineering, M. I. T.* (1957).
2) Danckwerts, P. V., *Trans. Instn. Chem. Engrs.*, **32**, 49 (1954).
3) Danckwerts, P. V., *Trans. Instn. Chem. Engrs.*, **32**, S53 (1954).
4) Danckwerts, P. V., *Trans. Faraday Soc.*, **46**, 300 (1950).
5) Fuller, E. C. and R. H. Crist, *J. Amer. Chem. Soc.*, **63**, 1644 (1941).
6) Fujita, S., *Chem. Eng. (Japan)* **18**, 73 (1954).
7) Gilliland, E. R. and T. K. Sherwood, *Ind. Eng. Chem.*, **26**, 516 (1934).
8) Higbie, R., *Trans. Am. Instn. Chem. Engrs.*, **31**, 365 (1935).
9) Hatta, S., *Technical Reports, Tohoku Imp. Univ.*, **10**, 613 (1932).
10) Lewis, W. K. and W. G. Whitman, *Ind. Eng. Chem.*, **16**, 1215 (1924).
11) Lightfoot, E. N., *A. I. Ch. E., Journal*, **8**, 710 (1962).
12) Matsuyama, T., *Chem. Eng. (Japan)* **14**, 249 (1950).

13) Yamaguchi, I., T. Oishi, N. Hashimoto and S. Nagata, *Mem. Fac. Eng.* (Kyoto Univ.) **27**, No. 1, 118 (1965).
14) Nagata, S. and I. Yamaguchi, *Chem. Eng.* (*Japan*) **24**, 726 (1960).
15) Saito, H. and H. Fukube, Read at *The Meeting of Chem. Eng. Soc.* (*Japan*) at Hamamatsu, Oct. (1962).
16) Toor, H. L., *A. I. Ch. E., Journal*, **4**, 97 (1958).
17) Van Krevelen, D. W. and P. J. Hoftijzer, *Recueil des Travaux Chemiques des Pays-Bas.*, **67**, 583 (1948).
18) Yamaguchi, I., *Chem. Eng.* (*Japan*) **26**, 595 (1962).